Modeling of Energy Transfer From Vibrationally Excited CO2 Molecules: Cross Sections and Probabilities for Kinetic Modeling of Atmospheres, Flows, and Plasmas

ARTICLE *in* THE JOURNAL OF PHYSICAL CHEMISTRY A · OCTOBER 2013

Impact Factor: 2.69 · DOI: 10.1021/jp408522m · Source: PubMed

4 AUTHORS:

Andrea Lombardi
Università degli Studi di Perugia
60 PUBLICATIONS **558** CITATIONS
SEE PROFILE

Noelia Faginas Lago
Università degli Studi di Perugia
48 PUBLICATIONS **252** CITATIONS
SEE PROFILE

Leonardo Pacifici
Università degli Studi di Perugia
68 PUBLICATIONS **394** CITATIONS
SEE PROFILE

Alessandro Costantini
INFN - Istituto Nazionale di Fisica Nucleare
44 PUBLICATIONS **118** CITATIONS
SEE PROFILE

THE JOURNAL OF PHYSICAL CHEMISTRY A

Article

pubs.acs.org/JPCA

Modeling of Energy Transfer From Vibrationally Excited CO_2 Molecules: Cross Sections and Probabilities for Kinetic Modeling of Atmospheres, Flows, and Plasmas

Andrea Lombardi,* Noelia Faginas-Lago, Leonardo Pacifici, and Alessandro Costantini

Dipartimento di Chimica, Università di Perugia, via Elce di Sotto 8, 06123 Perugia, Italy

ABSTRACT: We present extended applications of an established theoretical and computational machinery suitable for the study of the dynamics of CO_2+CO_2 collisions, focusing on vibrational energy exchange, considered over a wide range of energies and rotational temperatures. Calculations are based on quasi-classical trajectories on a potential energy function (a critical component of dynamics simulations), tailored to accurately describe the intermolecular interactions, modeled by the recently proposed bond−bond semiempirical formulation that allows the colliding molecules to be stretchable, rather than frozen at their equilibrium geometry. In a previous work, the same potential energy surface has been used to show that modifications in the geometry (and in physical properties such as polarizability and charge distribution) of the colliding partners affect the intermolecular interaction and determine the features of the energy exchange, to a large extent driven by long-range forces. As initial partitioning of the energy among the molecular degrees of freedom, we consider the excitation of the vibrational bending mode, assuming an initial rotational distribution and a rotational temperature. The role of the vibrational angular momentum is also carefully assessed. Results are obtained by portable implementations of this approach in a Grid-computing framework and on high performance platforms. Cross sections are basic ingredients to obtain rate constants of use in advanced state-to-state kinetic models, under equilibrium or nonequilibrium conditions, and this approach is suitable for gas dynamics applications to plasmas and modeling of hypersonic flows.

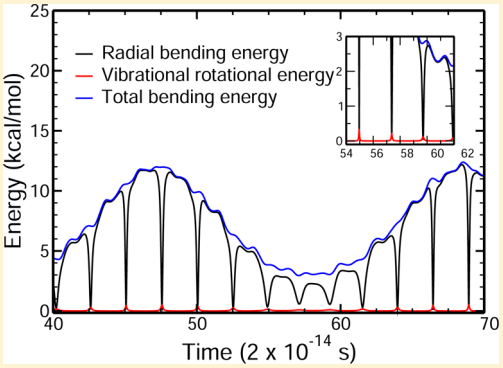

1. INTRODUCTION

The formation of highly vibrationally excited molecules under conditions of high temperature and pressure, typical of plasmas or hypersonic flows,[1] is mainly due to energy exchange during collisions. The most investigated typical exchange is the one occurring between the vibrational degrees of freedom of identical molecules (VV exchange), e.g., $N_2^*(v = 1) + N_2(v = 0) \rightarrow N_2(v = 0) + N_2^*(v = 1)$ or $CO_2(0\ 0\ 1) + CO_2(0\ 0\ 0) \rightarrow CO_2(0\ 0\ 0) + CO_2(0\ 0\ 1)$. Multiquantum VV exchange between the vibrational degrees of freedom of the molecules is also possible, though often considered to be less efficient. The dynamics of molecules in gaseous systems is indeed dominated by bimolecular collisions, which generate, besides VV energy transfer, also a significant roto-vibrational and translational energy exchange, from which the final global energy relaxation and the state population of molecules arise. From the point of view of the chemical reactivity, vibrationally excited molecules can dissociate, isomerize, or pump energy into endoergic processes. Accordingly, energy-relaxing and population-altering effects associated with inelastic bimolecular collisions play a key role in determining the energy balance of a variety of chemical processes. For this reason, the detailed study of the gas phase collision dynamics of pairs of identical molecules that are relevant to atmospheric chemistry, combustion, and plasma chemistry is the current object of a widespread attention from the scientific community. Among these processes, those involving carbon oxides, such as $CO_2 + CO_2$ and $CO + CO \rightarrow C + CO_2$, have relevance in the study of Earth's and planetary atmospheres[2,3] (their presence on Venus and Mars is well documented) but also in astrochemistry, since carbon compounds, e.g., carbon monoxide, are now known to be present in interstellar space. Recently, CO molecules have even been found in the 10-million-degree gas associated with the young supernova remnant Cassiopeia A (Cas A, see ref 4).

Besides their role in astrochemistry and atmospheric chemistry, the above-mentioned collision processes are an important part of the kinetic study of plasmas and gas flows, and of all the related gas dynamics applications. Indeed, the production of detailed inelastic molecular collision data to feed extended databases of state-to-state cross sections and rate coefficients is a recently developing area of research, motivated by the need of the gas dynamics community to improve the traditional approaches to kinetics and fluid dynamics models by including a description of the energy exchange and reactive processes at a state-to-state level of detail. This need is of particular interest for the study of gas flows and shock waves in connection with the spacecraft reentry problem (see the FP7 EU project[5]). Within this scope, energy exchange (mainly VV)

Received: August 26, 2013
Revised: October 7, 2013
Published: October 14, 2013

is a key issue, especially in those cases in which the speed of the vehicles exceeds the local speed of sound, with the consequent formation of a shock wave that leads to strong excitation of the molecular internal degrees of freedom (rotational, vibrational, and electronic) and promotes a large energy transfer and activation of many chemical reactions.[6] The peculiarity of these applications stems from the fact that reacting gaseous mixtures or plasmas, when interacting with the surface of the shield, are often characterized by thermal and chemical nonequilibrium conditions. The usual approach of averaging observables over an assumed known distribution (e.g., Boltzmann) is no longer valid and the appropriate observable, to be used in modeling, is the detailed collision cross section (a quantity, which is not averaged over a given energy distribution).

Weak noncovalent intermolecular interaction forces[7,8] deeply affect molecular collisions and intermolecular energy transfers. Therefore, detailed information on these interactions are a prerequisite for a realistic theoretical study of the inelastic collisions.[7,8] However, even for relatively simple systems, high level *ab initio* calculations of the intermolecular forces are computationally so demanding that an adequate investigation of the full configuration space is still, in practice, out of reach. Fortunately, a realistic description of these forces can be achieved using semiempirical approaches, which are so far the only viable alternative. In this perspective, an effective semiempirical formulation of the intermolecular interaction potential is that based on the so-called bond−bond approach (see ref 9 and references therein), in which the intermolecular interaction is expressed in terms of bond properties and parameters characterizing the internal molecular structure, such as charge distributions and polarizabilities.[10] The resulting parametrization of the interaction expresses the potential energy in terms of quantities having a well-defined physical meaning. It is, therefore, portable in different environments and conditions, being also extensible to systems of increasing complexity (see, for instance, refs 11−16).

For the case of the CO_2 + CO_2 collisions treated in ref 10, the effect of the excitation of vibrations and rotations has to be included in models, because polarizabilities and charge distributions, the properties more strictly related to intermolecular interactions, strongly depend on the internal motions of the interacting molecules. In turn, any modification of these physical quantities also induces significant variations in the intermolecular forces. In this respect, the work presented in ref 10 represents an improvement over the existing CO_2 dimer PESs (see, e.g., ref 17), obtained by releasing the constraint of frozen stretching and bending for the CO_2 monomers. This has also been confirmed in the same reference,[10] where a comparison of two calculations, one of which omits vibrational dependence, indicates that the inclusion of the effects of the molecular vibrations can strongly affect the final vibrational distribution of the products of the collisions. The resulting intermolecular part of the PES (which has been given a flexible analytic formulation including the dependence on the internal degrees of freedom (stretching and/or bending) of the monomers) is a basic ingredient of the method applied here, since it can be easily used in conjunction with computational technologies, which nowadays make available an impressive amount of computing time, by composing workflows of distributed applications in a Grid Empowered Molecular Simulator (GEMS), implemented on the Grid[18−21]).

In this paper, we shall consider the case of vibrational energy transfer in CO_2 + CO_2 collisions, for a set of specific transitions and over a range of collision energy and different rotational temperature values. In particular, the case of CO_2 molecules with initial bending excitation is investigated, with this work intended as the first of a series of studies devoted to investigating the energy transfer systematically for each vibrational mode. The results have all been obtained through a workflow for simulations of CO_2 + CO_2 collisions that has recently been developed as part of the activities of the virtual organization COMPCHEM.[22]

The remainder of the paper is organized as follows. In the next section, background information on the modeling of the interactions by the bond−bond approach to the intermolecular PES is given and the application to the case of CO_2 + CO_2 collisions is illustrated, together with details of the trajectory calculations. This is followed by a section in which a treatment of the vibrational angular momentum is illustrated and applied and results of calculations of cross sections and probabilities for a set of vibrational transitions upon collisions over a range of collision energies and at different rotational temperatures are presented. The last section contains a summary and an outlook to future perspectives.

2. THEORETICAL METHODS

2.1. Potential Energy Surface. The energy exchange between molecules is strongly dependent on the intermolecular interactions, whose accurate description is the main input of any scattering calculation based on models built with the purpose of obtaining energy transfer cross sections and rates. Indeed, the potential energy of a system of colliding molecules can be considered as a sum of two main contributions. One is the potential energy of the molecules when they are at infinite separation and is a unique function of the internal coordinates; the other is the contribution arising when the colliding partners are at a finite separation. At large distances (greater than typical bond distances), long-range attractive interaction dominates, whereas at short distances, the repulsive forces may overcome the attraction. During the collision, the combined effect of these attractive and repulsive noncovalent forces can induce internal distortions causing the exchange of energy among the translational, vibrational, and rotational degrees of freedom. Accordingly, an appropriate representation of a the potential energy surface (PES) for the study of the inelastic collisions is obtained expressing the interaction potential as a sum of an intramolecular term V_{intra}, depending on the internal coordinates of the two monomers, collectively denoted as $\{\mathbf{r}\}$, and of an intermolecular part V_{inter}, which is a function of the distance R between the centers of mass of the monomers, and of a set of angles defining the mutual orientation of the two interacting molecules, here collectively denoted as Ω. In addition, since the intermolecular interaction depends on physical properties of the two interacting molecules, such as charge distribution and polarizability, which in turn depend on the internal coordinates, the term V_{inter} must also be a function of $\{\mathbf{r}\}$:

$$V(R, \Omega, \{\mathbf{r}\}) = V_{intra}(\{\mathbf{r}\}) + V_{inter}(R, \Omega; \{\mathbf{r}\}) \quad (1)$$

In the above equation the internal interaction energy $V_{intra}(\{\mathbf{r}\})$ coincides with the potential energy of the two isolated molecules.

The term $V_{inter}(R,\Omega;\{\mathbf{r}\})$, a key player for the control of inelastic collisions, can be conveniently expressed as a sum of two effective interaction components:

dx.doi.org/10.1021/jp408522m | J. Phys. Chem. A 2013, 117, 11430−11440

$$V_{inter}(R, \Omega; \{\mathbf{r}\}) = V_{vdW}(R, \Omega; \{\mathbf{r}\}) + V_{elect}(R, \Omega, \{\mathbf{r}\}) \quad (2)$$

where V_{vdW} and V_{elect} represent the van der Waals (size repulsion plus dispersion attraction) and the electrostatic interaction components, respectively. V_{elect} originates from the anisotropic molecular charge distributions of the two bodies and tends to the permanent quadrupole−permanent quadrupole interaction at large distances. These two interaction energy terms vary strongly with the distance R between the centers of mass of the two monomers (e.g., the molecules a and b), but also show a weaker dependence on the additional coordinates (the Ω coordinates in eq 1) defining their mutual orientation.

Many alternatives choices are available for adopting a set of angular coordinates, preferably the ones resulting in a compact analytic expression of the PES and an intuitive connection with the geometrical properties of the system, especially when the focus is on the stereochemistry of the collision processes.[23−29] Compact expansions can be obtained in terms of special angular functions (i.e., hyperspherical harmonics[30−38]), following, for example, procedures most often used in quantum and classical mechanics to improve the separability of the internal degrees of freedom of molecules or clusters (see, e.g., ref 39).

Since the $V_{intra}(\{\mathbf{r}\})$ terms of eq 1 is the PES of the two isolated molecules, in the present work we used a potential function for the PES of the CO_2 molecule based on a many-body type representation of a potential due to Carter and Murrel.[40]

2.2. Bond−Bond Approach to the van der Waals Interaction Term. The bond−bond approach for the modeling of the intermolecular interactions has been illustrated in previous works (see ref 9 and references therein) and has been applied to the case of CO_2−CO_2 dimer interactions.[10] Here, we recall some background information and we refer to the work in ref 10 for a full account of the CO_2−CO_2 dimer case. The van der Waals term of the interaction of two molecules can be described as a sum of pairwise contributions, where the pairs are formed considering all the relevant interacting centers of each monomer. The interacting centers can be atoms (the most elementary choice), groups of atoms, or bonds, depending on the structure and dimension of the molecules and on the degree of accuracy that has to be ensured in the description of the interaction. The choice of single bonds as interacting centers is however the most accurate, since in these cases the corresponding bond polarizability, the physical quantity that is more directly connected to the intermolecular interactions, is well-defined and gives the best description of the properties of the bond. The van der Waals term, V_{vdW} of eq 2, is then expressed as follows:

$$V_{vdW}(R, \Omega) = \sum_{i}^{N} V^{i}_{vdW}(R_i, \omega_i) \quad (3)$$

(we for simplicity omitted the dependence on the internal coordinates $\{\mathbf{r}\}$ of the two molecules) The coordinate R_i is the distance between the reference points of the two interacting centers of the i-th pair, ω_i denotes collectively the angular coordinates defining the related mutual orientation of the interacting center (not needed if atoms are taken as interacting centers), and N is the number of interacting pairs. The V^{i}_{vdW} term represents the i-th pair interaction contribution, formulated as an extension and a generalization of the atom−bond pairwise interaction terms discussed in refs 41,42 in order to exploit their additive character. This kind of approach relies on long-standing research activity on interatomic potentials for rare-gas dimers, which includes, for example, several multi-parameter models,[43−47] the extensively used Hartree−Fock dispersion model[48,49] and subsequent modifications, and the Tang and Toennies model.[50] These models are difficult to apply to more complex cases, such as the present one, since too many parameters are involved in the representation.

The single V^{i}_{vdW} terms are calculated using the so-called Improved Lennard-Jones (ILJ) formula, defined in ref 51

$$\frac{V^{i}_{vdW}(R_i, \omega_i)}{\varepsilon_i(\omega_i)} = f(x_i) = \left[\frac{m}{n(x_i) - m} \left(\frac{1}{x_i} \right)^{n(x_i)} - \frac{n(x_i)}{n(x_i) - m} \left(\frac{1}{x_i} \right)^{m} \right] \quad (4)$$

where x_i is a reduced distance defined as

$$x_i = \frac{R_i}{R_{mi}(\omega_i)} \quad (5)$$

and ε_i and R_{mi} are respectively the well depth and the related equilibrium distance of the interaction potential. The parameter m takes pair specific values (e.g., the value is equal to 6 for neutral interacting centers). The above formula is indeed an extension and a generalization of the well-known pairwise potential function proposed by Maitland and Smith.[52] It is worth emphasizing here that the ILJ function[51] is definitely more realistic than the original Lennard-Jones (LJ(12,6)) one, because it represents more accurately both the size repulsion (first term within the square brackets) and the long-range dispersion attraction (second term within the square brackets).[34,53]

The exponent n in eq 4 is expressed as a function of both the distance R_i and the angles ω_i (see eq 3) by the following empirical equation:[42]

$$n(x_i) = \beta + 4.0 x_i^2 \quad (6)$$

in which β is a parameter depending on the nature and the hardness of the interacting centers that some way introduces the metric of a more ambient-like characteristic (the hardness of the interacting partners[42,51]), because it modulates the repulsion and controls the strength of the attraction.

The physical arguments that justify such a representation are based on the additive character of the bond polarizabilities in contributing to the overall molecular polarizability (a fundamental feature of the vdW interactions) a further advantage being that the bond polarizability, which is not merely the sum of the polarizabilities of the individual atoms, indirectly accounts for nonlinear three body effects.[41] The link between the well depth and position parameters (appearing in the V_{vdW} interaction terms) and the bond polarizabilities stems from a well established wealth of correlation rules, which summarize an ample phenomenology available on interatomic and intermolecular forces coming from spectroscopy and molecular beam scattering experiments, with the assistance of quantum chemistry calculations. For a full account on these aspects see ref 54 and references therein.

Following this approach, the main parameters characterizing each interaction center (assumed to be independent subunits having a definite polarizability and a given electronic charge distribution) are portable and can be used, usually with only

minor refinements, for the description of different or even larger interacting molecule systems.[14,15]

The relevant point for us is that the above formulation can be extended to the case of the interaction of nonrigid molecules. The variations of the bond lengths and angles characterizing the internal molecular motion lead, in fact, to corresponding variations of bond polarizabilities and point charge positions (and then of the interaction parameters), so changing the nature of the van der Waals and electrostatic components. This dependence can be made explicit in the analytic formulation of the potential energy surface, giving a flexible-monomer intermolecular potential.[10]

2.3. Electrostatic Component. The V_{elect} term of eq 2 can be formulated as a sum of Coulomb potential terms for each pair of interacting molecules, say a and b. For a given pair one has

$$V_{elect}(R, \Omega, \{\mathbf{r}\}) = \sum_{jk} \frac{q_{ja} q_{kb}}{r_{jk}} \tag{7}$$

where q_{ja} and q_{kb} are point charges located on the interacting molecules a and b and r_{jk} is the distance between them. The set of r_{jk} distances depends on the distance R and the angular variables Ω (and the internal coordinates). In the above given eq 7, the charge distributions on each molecular monomer are compatible with the corresponding calculated molecular quadrupoles.

Such formulation of V_{elect} improves the interaction description in those cases in which the molecular dimensions are not negligible with respect to the intermolecular distance R.[8] The choice of the spatial distribution of the charge is not a difficult task for relatively simple molecules (e.g., triatomics), especially when the dominance of strongly charged atoms (e.g., oxygen in H_2O) is apparent.[55−57] Such a choice, instead, becomes difficult (and to a certain extent also arbitrary) for more complex systems (see, e.g., refs 58,59).

2.4. Intermolecular Interaction of the CO_2 + CO_2 System. Both the V_{vdW} and V_{elect} terms of eq 2 depend, as mentioned above, on the distance R between the centers of mass of the two molecules (say a and b), and on a set of angular coordinates, that can be conveniently set up to be the Jacobi angular coordinates Θ_a, Θ_b, and Φ describing the $a-b$ mutual orientation as well (for examples about the role of the coordinate choice for the representation of the interactions, see[60,61] and references therein). The previous eq 3 becomes

$$V_{vdW}(R, \Theta_a, \Theta_b, \Phi) = \sum_{i}^{K} V^{i}_{vdW}(R_i, \theta_{ai}, \theta_{bi}, \phi_i) \tag{8}$$

in which R_i is again the distance between reference points conveniently placed on the two bonds of the i-th pair (denoted collectively as ω_i in eq 3, while θ_{ai}, θ_{bi}, and φ_i are the related mutual orientation angles for the i-th pair, and $K = 4$ is the number of CO−CO pairs characterizing the interaction of two CO_2 molecules. This formula is valid by virtue of the additivity of the various bond polarizability components, which contribute to form the overall molecular polarizability (a fundamental feature of the vdW interactions).

Important assumptions about the CO bonds considered as interacting centers are that each of them is treated as an independent diatomic subunit having a definite polarizability and electronic charge distribution of nearly cylindrical symmetry. It has also been assumed that the reference point of each bond is set at about the geometric bond center (more precisely the reference point of the CO pair has been displaced of 0.1278 Å toward the O-end) because the dispersion and the bond centers do not usually coincide.

The final step toward a flexible formulation of the V^{i}_{vdW} terms is to expand the parameters ε_i and R_{mi} in terms of bipolar spherical harmonics $A^{L}{}_{1}{}^{L}{}_{2}{}^{L}(\gamma)$.[10] In this way $f(x_i)$, the reduced form of the bond−bond potentials (see ref 42) is taken to be the same for all the relative orientations (see refs 62−65). For the CO_2-CO_2 system it was found sufficient to truncate the expansion to the fifth order. This implies that if one knows the $f(x_i)$ as a function of R_i for some specific configurations (five, in this case, corresponding to different mutual orientations of the two interacting molecules) the coefficients of the $A^{L_1L_2L}(\gamma)$ functions appearing in the expansion of the V^{i}_{vdW} term parameters can be obtained as the solution of a system of linear equations, for each value of R_i. A method to estimate the ε_i and R_{mi} expansion parameters from the values of bond (or diatomic molecule) polarizability is illustrated in detail in the Appendix A of ref 9 and in ref 66.

2.5. Quasi-Classical Trajectory Calculations. The trajectory calculations were performed on a potential energy surface that incorporates the potential energy function of the isolated molecules (V_{intra})[40] and the intermolecular potential function V_{inter} (see previous sections) developed according to the bond−bond approach illustrated above.[10] Calculations were carried out using the VENUS96 code[67] customized to include the above-mentioned PES and to properly sample initial conditions. The initial conditions of the trajectories run for our study were, in fact, selected as follows: the collision energy E was given a fixed value; the values of the initial rotational angular momenta of the two molecules, were selected through a random sampling of the Boltzmann distribution corresponding to the chosen rotational temperature T_{rot}, and the corresponding vectors $\mathbf{j}_a$ and $\mathbf{j}_b$ were randomly oriented; the initial vibrational states of the two molecules were defined by choosing two triples of integer numbers (one for each molecule) corresponding to the $v_{a(b)1}$, $v_{a(b)2}$, $v_{a(b)3}$ quantum numbers, and the vibrational angular momentum quantum number was disregarded. Then, initial coordinates and momenta for the relative motion were set by assigning a random value to the impact parameter b in the range $[0,b_{max}]$, with b_{max}, the maximum impact parameter, being taken as a truncation limit. The molecules were then randomly oriented, with the initial intermolecular distance set large enough to make the interaction between them negligible and the rotation of each of them that of a linear rigid rotor, with no coupling between rotations and vibrations.

Batches of 50 000 trajectories were run for each pair of energy and rotational temperature and for each pair of triples of initial vibrational states, by setting the maximum impact parameter b_{max} equal to 20 Å (so as to get full account of the effects of the long-range tail of the intermolecular interactions).

After running any given batch of trajectories, the set of continuous classical final vibrational energies of the molecules was binned as for initial conditions, using a separable normal mode harmonic model. As a matter of fact, the energies corresponding to each normal mode were calculated by projecting the phase-space vector of the system final states into the CO_2 normal mode vector basis. It is expected that this quantization method, by far the most commonly used in the quasi-classical trajectory method treatment of collision dynamics, spurs some inaccuracy in the labeling of the

vibrational states for highly excited molecules. This is, however, of negligible impact on our study, because the collision product molecules, at the considered energies, are unlikely to access the strong anharmonic region and rather evolve down to the lowest region of the intramolecular potential energy surface. One can indeed estimate approximately the deviations of the harmonic model from the actual behavior of the system by simply comparing the harmonic vibrational energy levels of CO_2, for a single mode of vibration, with the ones associated with the same vibrational state of the corresponding standard Morse potential (for example, the energy difference for $v_1 = 11$ (symmetric stretching) is about 10%; see ref 10). Moreover, it is important to point out here that such deviations do not invalidate the use of the normal mode harmonic model under thermal conditions. In fact the assignment of a final classical state to a quantum one is only instrumental to the setting of an integration energy grid for the evaluation of a thermally averaged property. In other words, a difference in the labeling of the states on which the thermal average is performed changes only the sampling of the numerical integration points without affecting the final estimate of the integral. Attention has only to be paid when dealing with the evaluation of detailed properties in which a rigorous correspondence between states and energy values need to be adopted.

The initial rotational states of the colliding molecules, for the various trajectory runs, were sampled from a Boltzmann distribution characterized by a given value of rotational temperature. This sampling of rotational energies is equivalent to the choice of running trajectories with specified vibrational energies of the colliding partners, but averaged over rotational states (according to the given rotational temperature). This choice is motivated by the fact that different collision-induced energy exchange processes occur on different time-scales and with different rates in gas phase, when a gas tends to relax into equilibrium (that is exactly the situation in which usually state-to-state cross sections are used for modeling). It is therefore justified to consider vibrational state-to-state probability cross sections and rates as rotationally averaged relying on the fact that rotation−rotation and vibration−vibration energy transfers take place over significantly different time scales and there is, accordingly, a sufficiently long interval of time for the entire manifold of rotational states (belonging to a given vibrational state) to reach the equilibrium. The rotational temperature T_{rot} at which each state-to-state cross section and the related quantities result to be average is set at a value equal to that of the translational temperature, as usually done for this type of massive computational campaign. Also this assumption relies on the time scale argument: in a gas tending to equilibrium (also locally) the energy transfer to translation from other degrees of freedom is in general the slowest process, and eventually energy allocated in any degrees of freedom will tend to be in equilibrium with the translations. This choice of considering rotationally averaged quantities creates the problem of averaging the cross sections at various values of the fixed rotational temperature. In fact, in case one is interested in state-to-state rate constants, as is usual in kinetic modeling, the cross section has to be averaged over a given energy (velocity) distribution, at a given temperature. This implies that, in principle, cross sections should be evaluated at as many rotational temperatures as the ones at which the corresponding rate constants have to be obtained. A reasonable compromise, avoiding excess calculations, is that of selecting a reduced number of rotational temperatures, for each set of initial conditions.

The probability P_v for a given vibrational state change upon collision is the ratio of the number of transition trajectories to the total number of trajectories $(N_v/(N_t))$, while the related cross section σv is defined, as usual, as

$$\sigma_v = \pi b_{max}^2 \frac{N_v}{N_t}$$

The main drawback of classical trajectories of generating vibrational state energies falling below the zero-point energy is partially corrected by simply discarding those trajectories which are not permitted according to quantum theory.

3. RESULTS AND DISCUSSION

3.1. Vibrational Energy Transfer in CO_2 Collisions. The evaluation of the energy exchange occurring in molecular collisions between external (translation) and internal (rotation, vibration) degrees of freedom is a direct effect of the intermolecular interactions. The energy transfer also depends on the initial allocation of the energy among the degrees of freedom of the colliding molecules, since the polarizabilities and multipole moments can vary significantly with the vibrational and/or rotational excitation of the molecules. The importance of molecular vibrational energy gains or losses is associated with the fact that they have, as already mentioned, a significant impact on the reactivity of the chemical species, because the breaking and formation of chemical bonds is enhanced by the energy transfer to and from the vibrational degrees of freedom of a molecule. Here we focus on the VV transfer occurring in CO_2−CO_2 collisions by considering the state-to-state probabilities and cross sections for the following class of processes:

$$CO_2(v_{a1}, v_{a2}, v_{a3}) + CO_2(v_{b1}, v_{b2}, v_{b3}) \rightarrow CO_2(v_{a1}', v_{a2}', v_{a3}') + CO_2(v_{b1}', v_{b2}', v_{b3}') \quad (9)$$

where the $v_{a(b)i}$ $(i = 1, 2, 3)$ are the quantum labels of the three vibrational modes of CO_2. These quantum numbers correspond to the symmetric stretching, bending, and asymmetric stretching, respectively, before (unprimed) and after (primed) the collision event involving the two (a and b) CO_2 molecules. The bending mode of CO_2 is degenerate since the molecule has a linear geometry. When the bending mode is excited, rotation around the O−C−O molecular axis may occur and an additional (l) quantum number is needed to label the discretized total molecular angular momentum projection on the quantization axis, say z. The explicit treatment of rotations around the C_∞ symmetry axis of the CO_2 molecule (two additional degrees of freedom, one per molecule) can lead to significant increase of the computing load, especially when one is dealing with systematic studies of state-to-state cross sections. Such a higher dimensionality investigation is however very useful in order to assess the role played by the vibrational angular momentum in determining the fate of CO_2−CO_2 collisions.

3.2. Vibrational Angular Momentum and Vibrational Rotation Energy. The two degenerate bending degrees of freedom can be conveniently treated as a two-dimensional oscillator and the corresponding normal coordinate can be represented in terms of polar variables. Let us suppose the z axis of the molecular body frame coincides with the C_∞ symmetry axis of the linear CO_2 molecule and denote as ξ_x

and ξ_y the orthogonal components of the two-dimensional bending mode of vibration. These components can be expressed in terms of a radius ρ and angle θ ranging from 0 to 2π, as follows:

$$\xi_x = \rho\cos\theta \qquad (10)$$

$$\xi_y = \rho\sin\theta$$

with $\rho^2 = \xi_x^2 + \xi_y^2$. In classical mechanics, the angular momentum L associated to the ξ's, in this case a vibrational angular momentum, can be obtained as

$$L = \dot{\xi}_x\xi_y - \xi_x\dot{\xi}_y$$

Consequently, the classical vibrational rotation energy E_l associated to the bending motion can be evaluated as

$$E_l = \frac{L^2}{2\rho^2} \qquad (11)$$

In terms of the above quantities, the total bending energy E_b associated to the bending mode, is the sum of a radial bending energy (radial kinetic and potential energy), plus the energy E_l associated with the vibrational angular momentum L, as follows:

$$E_b = \frac{1}{2}[\dot{\rho}^2 + \rho^2\omega^2] + \frac{L^2}{2\rho^2} \qquad (12)$$

where ω is the vibrational frequency of the degenerate bending mode. According to the standard derivation of normal mode coordinates as a combination of mass-scaled Cartesian coordinates, the ξ's of eq 10 have units of mass inside and this ensures the physical dimension of the quantities in eqs 11 and 12 to be that of an energy. Now, it must be pointed out that the amount of rotational energy around the C_∞ symmetry axis is expected to be small, both because most of rotations occur around the two perpendicular C_2 symmetry axes of the molecule, and because most of the time the molecule will have a geometry close to the linear one. This fact can be directly observed and verified by monitoring the time evolution of the bending energy E_b along with its radial and rotational (E_l) components. As a matter of fact, this is what one finds for a typical collision trajectory of a pair of CO_2 molecules, initially at the (0,3,0) and (0,0,0) vibrational states with a collision energy of 20 kcal/mol. Results are shown in Figure 1.

It can be seen that the radial and angular components of the bending energy periodically reach (in coincidence) a minimum and a maximum, as a function of time. These features of the time evolution plots correspond to the maximum elongation from the linear geometry that is reached by the CO_2 molecule during its bending oscillations and represents the amplitude of the bending motion. At the maximum elongation of bending from the equilibrium linear geometry, the rotation around the molecular C_∞ axis is enhanced and the purely radial motion (i.e., the variation of the module of the bending mode coordinates, considered as a two-dimensional vector) is at its minimum. Due to these considerations, in our model treatment of the CO_2 monomer, we find it reasonable to neglect the vibrational angular momentum quantum number, on the grounds that the associated amount of energy is in general small and, in any case, smaller than the statistical error of the trajectory averaged calculated quantities (that amounts up to 5%). To further confirm that the vibrational rotation energy can actually be safely disregarded in the collisions that we are considering here, we compare in Figure 2 the time evolution of E_l from Figure 1 with that of E_l from a collision trajectory with initial conditions identical to the previous ones, but with the molecules initially set at (0,10,0) and (0,3,0) vibrational states (a value of 10 for the quantum number of the bending mode, as well as for other modes, is an upper limit for the vibrational transitions in the range of collision energies considered here). As expected due to the higher energy content of the bending mode, increased values of E_l are observed, but still well below the value of 1 kcal/mol. This is an indication that, besides having negligible effects on the energy disposal into rotations

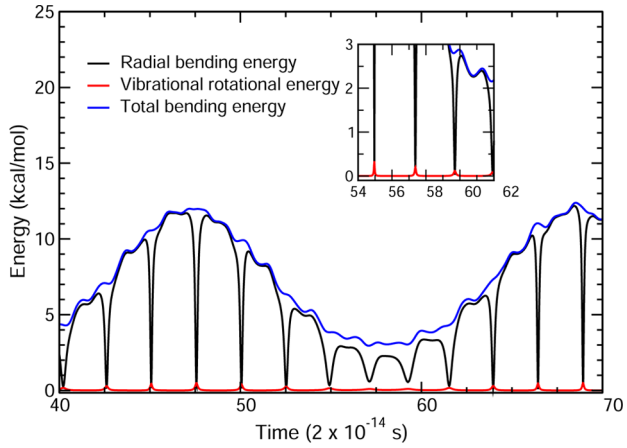

Figure 1. Time evolution of the total bending energy (blue line) and the corresponding radial (black line) and vibrational rotation (red line) components, during a collision with molecules initially in the (0,3,0) and (0,0,0) vibrational states. It can be clearly seen that the radial component almost entirely equals the total energy, while the rotational component is very small. The strong oscillations characterizing the radial and rotational component evolution are caused by the fact that the molecule periodically crosses the linear geometry, losing rotational degrees of freedom. The peaks of the rotational component, correspond to the maximum distance reached from the linear geometry (bending motion turning point).

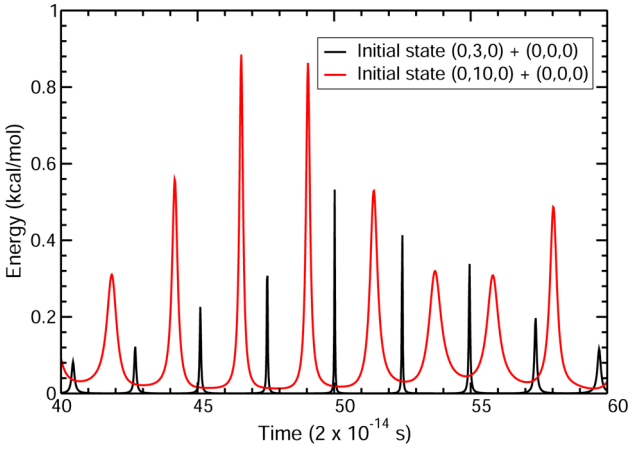

Figure 2. Time evolution of the vibrational rotation energy E_l for two different initial vibrational states of the colliding CO_2 molecules. The black line shows E_l as obtained when one of the molecules is initially in the (0,3,0) vibrational state, while the red line shows E_l when one of the molecules is initially in the (0,10,0) vibrational state, with a much higher energy content in the bending mode. Although higher values of the vibrational rotation energy are observed in this second case, the energy E_l is well below the value of 1 kcal/mol everywhere.

dx.doi.org/10.1021/jp408522m | J. Phys. Chem. A 2013, 117, 11430−11440

around the molecular internuclear axis, the vibrational angular momentum is negligible also in the process of sampling the initial conditions (at least in the considered energy and temperature regime). In fact, an initial component of this angular momentum can be generated by choosing the bending direction perpendicular to the plane of rotation of the molecule, but the trajectory results should not be significantly influenced by the choice of either a parallel or perpendicular direction of bending.

To allow separability between rotation and vibration degrees of freedom, thanks also to the outcome of the above analysis of the vibrational angular momentum, the CO_2 molecule can be approximated as a linear rotor (with only two rotational degrees of freedom) and the coupling between rotations and vibrations can be neglected, so corroborating the choice (accounted in the Theoretical Methods section above) of considering separable rotations and vibrations. Yet all the possible dynamical effects induced by the variation of the molecular shape as a consequence of the vibrational motion are properly taken into account by the intermolecular potential V_{inter} as explained above.

3.3. State-to-State Cross Sections and Probabilities for Collisions of CO_2 Molecules with Bending Mode Excited. In order to investigate the specific effect of the bending excitation of CO_2 in the energy transfer in CO_2-CO_2 collisions, we performed a set of calculations starting at values of the collision energy E ranging from 1 to 20 kcal/mol, setting, as already mentioned, each of the two molecules in a triple of initial vibrational states. In doing this, the vibrational angular momentum was neglected (as already anticipated above) and a set of pair of triples $(0,n,0)+(0,0,0)$, with n = 1, 2, 3, 4, 5, 6 was adopted (hereinafter we will adopt this notation to represent the initial vibrational state of a pair of CO_2 molecules). This is in order to have one molecule with the bending mode excited and the other in the ground vibrational state. The molecular rotational angular momentum $\mathbf{j}_{a(b)}$ was selected randomly according to a set o values of rotational temperatures T_{rot} = 1000, 2000, 3000 K, for the case n = 3, and according to T_{rot} = 1000 K for n = 1, 2, 4, 5, 6.

A first important indication on the interplay of the different vibrational modes in exchanging energy at moderately high energies is provided by Tables 1 and 2 in which we report the calculated values of the top 20 state-to-state vibrational energy transfer cross sections and related probabilities for each detected final vibrational state at a total energy E = 1 kcal/mol, rotational temperatures T_{rot} equal to 1000 and 2000 K, respectively, for the initial pair of triples (0,3,0) + (0,0,0). The values of the probabilities and cross sections listed in the tables show that in general when bending is excited, there is an efficient intramolecular transfer of energy to the symmetric stretching modes yet at such relatively low collision energy value. Such intramolecular transfer is efficient also into the same mode of the other molecule initially in its ground vibrational state. As expected, energy is also transferred to vibrations from rotational and translational degrees of freedom, with the initial vibrational energy of the colliding molecules, three bending quanta, not being conserved. These results confirm the fact that in triatomic molecules the bending and symmetric stretching modes strongly interact, even at relatively low energy values.[10] This is probably a manifestation of the fact that the energy of the first excited stretching state (1 0 0) is nearly the same as the energy of the second bending excited state (0 2 0), and so are their respective frequencies of vibration. This is a condition for a classical resonance (the analogue of the quantum Fermi resonance), which is at the base of the observed strong interplay between these two modes. We find, on the other hand, that the excitation of the highest frequency asymmetric stretching mode does not appear in the list of the most probable processes, suggesting that this mode is strongly decoupled from the other two (bending and stretching) and that a larger amount of energy is needed to

Table 1. Collision Probabilities and Cross Sections for Vibrational Transitions at Energy E = 1 kcal/mol, Molecular Angular Momenta Sampled from a Boltzmann Distribution with T_{rot} = 1000 K, for the Initial Pair of Vibrational States (0,3,0) + (0,0,0)

v_{a1}', v_{a2}', v_{a3}'	v_{b1}', v_{b2}', v_{b3}'	prob.	cross section (Å^2)
1 1 0	0 0 0	0.22162	280.0
1 1 0	1 0 0	0.17939	230.0
3 0 0	1 0 0	0.14702	220.0
2 1 0	1 0 0	0.09814	140.0
2 1 0	0 0 0	0.08813	120.0
4 0 0	1 0 0	0.07429	120.0
3 0 0	0 0 0	0.08648	115.0
4 0 0	0 0 0	0.03954	53.0
3 1 0	1 0 0	0.01440	22.0
3 1 0	0 0 0	0.01101	15.7
1 2 0	1 0 0	0.01161	14.8
2 0 0	1 0 0	0.00823	10.5
1 2 0	0 0 0	0.00509	6.8
2 0 0	0 0 0	0.00341	3.8
0 2 0	0 0 0	0.00262	2.7
0 1 0	0 0 0	0.00163	1.2
1 0 0	0 1 0	0.00170	0.93
2 0 0	0 1 0	0.00029	0.16
1 1 0	0 1 0	0.00024	0.07
3 0 0	2 0 0	0.00022	0.06

Table 2. Collision Probabilities and Cross Sections for Vibrational Transitions at Energy E = 1 kcal/mol, Molecular Angular Momenta Sampled from a Boltzmann Distribution with IT_{rot} = 2000 K, for the Initial Pair of Vibrational States (0,3,0) + (0,0,0)

v_{a1}', v_{a2}', v_{a3}'	v_{b1}', v_{b2}', v_{b3}'	prob.	cross section (Å^2)
3 0 0	1 0 0	0.16570	250.0
1 1 0	0 0 0	0.18703	240.0
1 1 0	1 0 0	0.19612	241.0
3 0 0	0 0 0	0.10598	150.0
2 1 0	1 0 0	0.09543	135.0
2 1 0	0 0 0	0.08551	122.0
4 0 0	1 0 0	0.04814	75.0
4 0 0	0 0 0	0.03510	49.0
2 0 0	1 0 0	0.02798	39.0
2 0 0	0 0 0	0.01614	22.0
3 1 0	1 0 0	0.00985	14.5
3 1 0	0 0 0	0.00763	10.4
1 2 0	1 0 0	0.00675	8.5
1 2 0	0 0 0	0.00244	3.2
0 2 0	0 0 0	0.00205	1.6
0 1 0	0 0 0	0.00102	0.73
2 0 0	0 1 0	0.00046	0.14
1 1 0	0 1 0	0.00024	0.11
1 0 0	1 0 0	0.00015	0.09
3 0 0	0 1 0	0.00027	0.08

dx.doi.org/10.1021/jp408522m | J. Phys. Chem. A 2013, 117, 11430−11440

collisionally activate the asymmetric stretching. Even at the highest collision energies considered here, the picture remains unchanged and a strong interplay of bending and symmetric stretching is observed, while the manifold of the asymmetric stretching excited states is not accessed. These results also confirm and extend the preliminary indications obtained from a previous study carried out to support and validate the choice of introducing flexibility (see the Theoretical Methods section) into the description of the intermolecular interaction energy of the colliding monomers.[10] The effect of changing the rotational temperature T_{rot} from 1000 to 2000 K also does not alter the essential of the energy transfer dynamics, even if it modifies significantly the relative probabilities and the cross section ranking for the most important transitions.

It is worth noting here that even at relatively low collision energies, several channels end up being non-negligibly populated by collision induced vibrational transitions, and the analysis of the complete set of transitions, not reported here, indicates that the value of the cross sections decreases in such a way that at least a few tens of possible final states correspond to probable transitions. Many other (on the order of thousands for the higher energies) are definitely less effective and the associated probabilities and cross sections would require a significantly larger number of trajectories to be accurately estimated. The main transitions listed in Tables 1 and 2 account cumulatively for nearly the 90% of the events taking place in collisions at the given energies and rotational temperatures. Many transitions representing minor channels have not been listed. The role of these channels, although appearing of secondary importance due to the low probabiities, cannot be in principle neglected in kinetic models of plasmas and gas flows, since the corresponding transitions in many cases populate the higher energy band of the accessible final vibrational states. We here omit these low-probability transitions, principally because the values of the corresponding cross sections are not accurate enough.

These aspects are better specified by inspecting, for a given set of most probable transitions, the plots of the collision probabilities as a function of the collision energy. Figure 3 below shows the trend of the probabilities for the indicated set of transitions (selected among the most probable ones) at T_{rot}

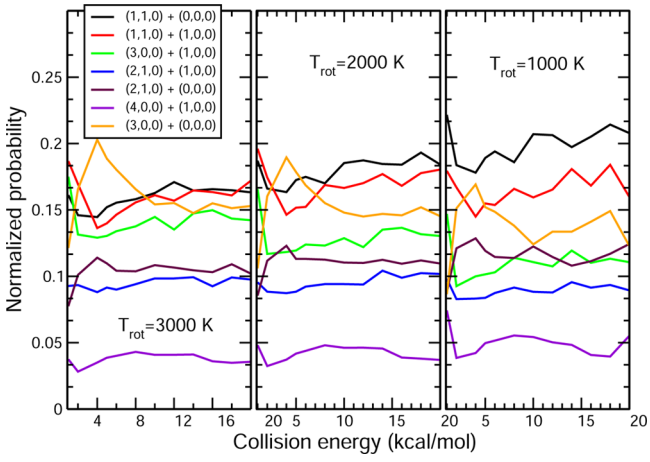

Figure 3. Probabilities as function of the collision energy for a series of vibrational transitions from initial vibrational states of colliding molecules (0,3,0) + (0,0,0) at rotational temperatures T_{rot} = 1000, 2000, 3000 K.

equal 1000, 2000, and 3000 K, respectively, as a function of the collision energy E. The plots indicate that, at least in the three cases considered here, the behavior of the given set of transitions does not substantially change with the rotational temperature. The dependence of the probability on the collision energy shows mainly weak oscillations over the interval of energy ranging between 1 and 20 kcal/mol, with no threshold effects for this kind of vibrational transitions under the considered conditions. On the contrary, the individual behavior of the transitions can slightly change for different rotational temperatures, as is the case, for example of the relative weight of the (1,1,0) + (0,0,0) and (3,0,0) + (0,0,0) transition in moving from T_{rot} = 1000 K to T_{rot} = 3000 K.

The energy transfer involving the vibrational degrees of freedom of CO_2, under the considered conditions, is dominated by the behavior of the bending and symmetric stretching modes, although the reported results do not allow to exclude that the vibrational energy exchange between molecules could be funneled by the combined effect of vibration−rotation and/or vibration−translation energy transfer. To partially disentangle the role of these effects, Figure 4 shows the average VV,

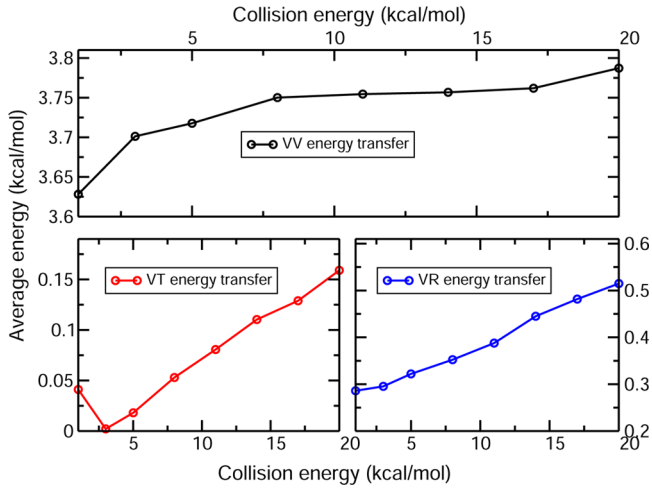

Figure 4. Average energy transfer among the various molecular degrees of freedom as a function of the collision energy E at T_{rot} = 1000 K, for collisions of CO_2 molecules initially in the (0,3,0) + (0,0,0) pair of vibrational states. Upper panel: vibration−vibration energy transfer. Lower left panel: vibration−translation energy transfer. Lower-right panel: vibration−rotation energy transfer.

vibration−rotation (VR), and vibration−translation (VT) average exchange energy in the collision energy interval ranging from 1 to 20 kcal/mol, for T_{rot} = 1000 K and initial pair of triples (0,3,0) + (0,0,0). As a matter of fact, the figure confirms that most of the energy transfer is due to direct vibration−vibration exchange, while little or no energy is transferred from or to the other molecular degrees of freedom. The mean value of the VV energy approximately ranges from 3.6 to 3.8 kcal/mol, a value similar to that of the energy corresponding to two bending energy quanta (~3.8 kcal/mol). It is expected, however, that higher rotational temperature would enhance considerably the VR exchange.

The trend of the state-to-state cross sections and probabilities appears to be more interesting when examined as a function of the initial vibrational excitation of the colliding molecules. Figure 5 shows the probabilities of the same set of most probable transitions (considered in previous Figure 3) as

dx.doi.org/10.1021/jp408522m | J. Phys. Chem. A 2013, 117, 11430−11440

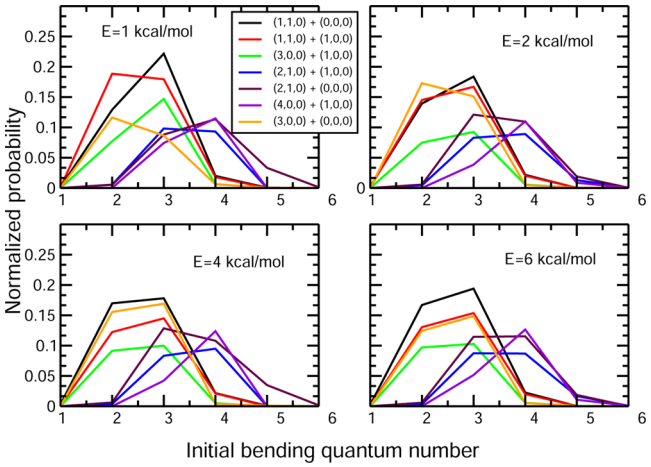

Figure 5. Normalized probabilities of a set of vibrational transitions upon CO_2 + CO_2 collisions, as a function of the initial bending quantum number n, for the initial pair of triples $(0,n,0)$ + $(0,0,0)$, with n = 1, 2, 3, 4, 5, 6. The probabilities are given at four different values of the collision energy E = 1, 2, 4, 6 kcal/mol.

a function of the initial bending quantum number n of the initial pair of triples $(0,n,0)$+$(0,0,0)$, for n = 1, 2, 3, 4, 5, 6 and for collision energies E = 1, 2, 4, 6 kcal/mol. From the plots, it can be seen that the given set of vibrational transitions is subjected to a similar trend for all the considered energy values. There is an increase of probabilities for increasing values of n, followed by a quenched trend at higher bending quantum numbers.

In Figure 6 the same type of data are considered, but for energies E = 14, 16, 18, 20 kcal/mol. The trend appears

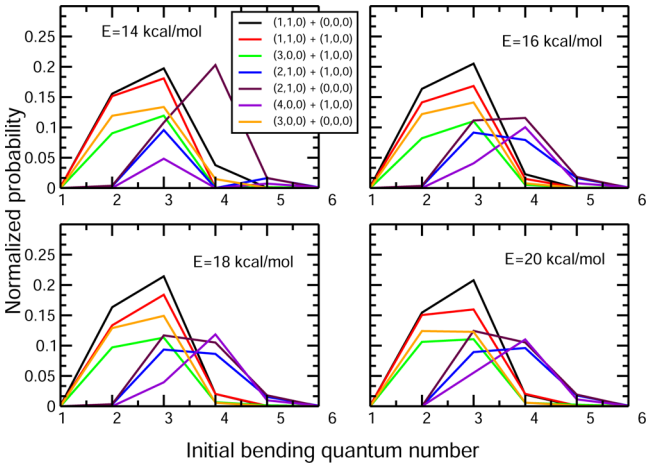

Figure 6. Normalized probabilities of a set of vibrational transitions upon CO_2 + CO_2 collisions, as a function of the initial bending quantum number n, for the initial pair of triples $(0,n,0)$ + $(0,0,0)$, with n = 1, 2, 3, 4, 5, 6. The probabilities are given at four different values of the collision energy E = 14, 16, 18, 20 kcal/mol.

substantially similar. This suggests that the set of probable VV transitions can be divided into a number of subsets characterized by a similar increasing−decreasing trend over a certain range of initial bending quantum numbers, with that range compatible with the typical average energy exchange characterizing the VV transitions of the subset.

A further confirmation of this fact can be obtained, from the available data, by analyzing the trend of probabilities as a function of the initial bending quantum number but for a different subset of vibrational transitions. Figure 7 shows the

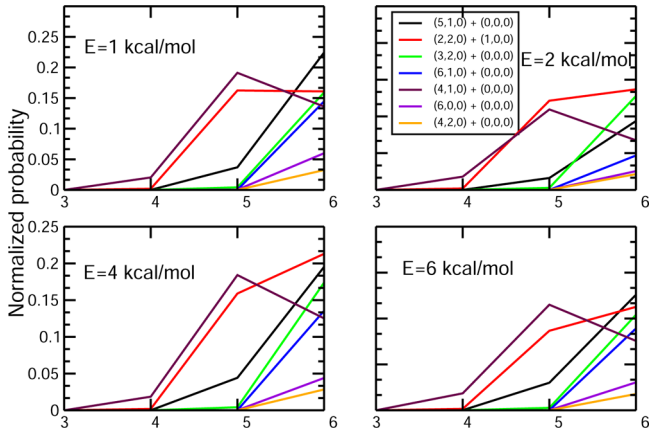

Figure 7. Normalized probabilities of a set of vibrational transitions upon CO_2 + CO_2 collisions, as a function of the initial bending quantum number n for the initial pair of triples $(0,n,0)$ + $(0,0,0)$, with n = 1, 2, 3, 4, 5, 6. The chosen set of vibrational transitions is different from the one considered in Figures 5 and 6. The probabilities are given at four different values of the collision energy E = 1, 2, 4, 6 kcal/mol.

trend of probabilities as a function of the initial bending quantum number of a different subset of transitions (which is reported in the figure). It can be seen that probabilities become non-negligible at n = 3, while although not entirely shown in the figure and only partially visible, the start of the subsequent decrease of probabilities is also present. Since data for higher quantum numbers, which are involved in the dynamics at higher energy ranges, are not yet available, a completely systematic study of these trends and features of VV probabilities and cross sections will be the object of future work.

4. CONCLUSIONS

In this paper we have reported and discussed a quasi-classical trajectory study of the dynamics of gas phase collision processes involving CO_2 molecules. Processes involving carbon dioxide are of interest in the modeling of earth and planetary atmospheres, plasmas, and gas flows. The target of the study is the calculation of probabilities, cross sections, and rates for the detailed molecular vibrational energy transfer processes, to be used in gas and plasma kinetic studies under a wide range of conditions and in the framework of a general state-to-state approach to molecular kinetics. The noteworthy point in the study is the extensive use of a potential energy surface that assembles intra- and intermolecular parts in which the description of the intermolecular forces is not limited to considering the molecules as rigid, but takes into account the dependence (not negligible) of these forces on stretching and bending vibrational modes. Such assemblage has been guided by the GEMS molecular dynamics simulator. The resulting computational tool grants accurate descriptions of the intermolecular interaction energy, based on a bond−bond semiempirical approach (the way to include the dependence of the interaction on the internal molecular degrees of freedom) and is suitable to exploit the massive usage of quasi-classical trajectories. This is the reason it is currently being implemented as a web service to be offered to the molecular science community on the Grid scientific portal by COMPCHEM. The

dx.doi.org/10.1021/jp408522m | J. Phys. Chem. A 2013, 117, 11430−11440

current test bed version of the tool has been widely used for the present application to the study of the CO_2+CO_2 vibrational energy transfer in nonreactive collisions.

A treatment of the vibrational angular momentum and of the associated vibrational rotation energy, to carefully assess its role in the VV energy transfer, has also been illustrated and implemented.

Our attention has been focused on collisions involving bending excited molecules, following the idea, to be pursued in further studies, of analyzing the VV energy transfer dynamics considering separately the initial excitation of the three vibrational modes of the carbon dioxide molecule. The results that have been shown here, coupled to those obtained from ongoing analogous systematic studies of the other vibrational modes, will provide insights into the energy transfer dynamics to be used as a guide in the construction of comprehensive nonequilibrium rate coefficient databases for energy exchange processes and reactions in gas phase, to be used in kinetic models of atmosphere, plasma, and hypersonic flows.

AUTHOR INFORMATION

Corresponding Author

*E-mail: ebiu2005@gmail.com.

Notes

The authors declare no competing financial interest.

ACKNOWLEDGMENTS

The authors acknowledge financial support from MIUR PRIN 2008 (contract 2008KJX4SN_003), MIUR PRIN 2010−2011 (contract 2010ERFKXL_002), Phys4entry FP72007−2013 (contract 242311) and EGI Inspire. Thanks are also due to IGI and the COMPCHEM virtual organization and to the Italian CINECA for the allocated computing time.

REFERENCES

(1) Capitelli, M.; Bruno, D.; Colonna, G.; D'Ammando, G.; Esposito, F.; Laricchiuta, A.; Pietanza, L. D. Molecular Physics and Kinetics of High-temperature Planetary Atmospheres. *Rendiconti Lincei* **2011**, *22*, 201−210.

(2) Khalil, M. A.; Rasmussen, R. A. Carbon Monoxide in the Earth's Atmosphere: Indications of a Global Increase. *Nature* **1988**, *332*, 242.

(3) Palazzetti, F.; Maciel, G. S.; Lombardi, A.; Grossi, G.; Aquilanti, V. The Astrochemical Observatory: Molecules in the Laboratory and in the Cosmos. *J. Chin. Chem. Soc.—Taip.* **2012**, *59*, 1045−52.

(4) http://www.astronomy.com/ /link.aspx?_id=9c5fef44-c7a0-4333-baeb-628add917d08.

(5) Project Phys4entry FP7242311, http://users.ba.cnr.it/imip/cscpal38phys4entry/activities.html.

(6) Capitelli, M.; Ferreira, C. M.; Gordiets, B. F.; Osipov, R. In *Plasma kinetics in atmospheric gases*; Springer Verlag, 2000.

(7) Hirschfelder, J. O. Intermolecular Forces. In *Advances in Chemical Physics*; Wiley: New York, 1967; Vol. *12*.

(8) Maitland, G. C.; Rigby, M.; Smith, E. B.; Wakeham, W. A. In *Intermolecular Forces*; Clarendon Press: Oxford, 1987.

(9) Cappelletti, D.; Pirani, F.; Bussery-Honvault, B.; Gomez, L.; Bartolomei, M. A bond-bond Description of the Intermolecular Interaction Energy: the Case of Weakly Bound N_2-H_2 and N_2-N_2 Complexes. *Phys. Chem. Chem. Phys.* **2008**, *10*, 4281−4293.

(10) Bartolomei, M.; Pirani, F.; Laganà, A.; Lombardi, A. A Full Dimensional Grid Empowered Simulation of the CO_2 + CO_2 Processes. *J. Comput. Chem.* **2012**, *33*, 1806.

(11) Bruno, D.; Catalfamo, C.; Capitelli, M.; Colonna, G.; De Pascale, O.; Diomede, P.; Gorse, C.; Laricchiuta, A.; Longo, S.; Giordano, D.; Pirani, F. Transport Properties of High-temperature Jupiter Atmosphere Components. *Phys. Plasmas* **2010**, *17*, 112315.

(12) Albertí, M.; Huarte-Larrañaga, F.; Aguilar, A.; Lucas, J., M.; Pirani, F. A 3D-analysis of Cluster Formation and Dynamics of the X-benzene (X = F, Cl, Br, I) Ionic Dimer Solvated by Ar Atoms. *Phys. Chem. Chem. Phys.* **2011**, *13*, 8251.

(13) Lombardi, A.; Faginas-Lago, N.; Laganà, A.; Pirani, F.; Falcinelli, S. A bond−bond portable approach to intermolecular interactions: simulations for N-methylacetamide and carbon dioxide dimers. *Lecture Notes Comput. Sci., Part 1* **2012**, *7333*, 387−400.

(14) Faginas-Lago, N.; Albertí, M.; Laganà, A.; Lombardi, A. Water (H_2O)m or Benzene (C_6H_6)n Aggregates to Solvate the K^+? *Lecture Notes Comput. Sci., Part 1* **2013**, *7971*, 1−15.

(15) Falcinelli, S.; Rosi, M.; Vecchiocattivi, F.; Bartocci, A.; Lombardi, A.; Faginas-Lago, N.; Pirani, F. Modeling the Intermolecular Interactions and Characterization of the Dynamics of Collisional Autoionization Processes. *Lecture Notes Comput. Sci., Part 1* **2013**, *7971*, 69−83.

(16) Lombardi, A.; Laganà, A.; Pirani, F.; Palazzetti, F.; Faginas-Lago, N. Carbon Oxides in Gas Flows and Earth and Planetary Atmospheres: State-to-State Simulations of Energy Transfer and Dissociation Reactions. *Lecture Notes Comput. Sci., Part 2* **2013**, *7972*, 17−31.

(17) Barton, A. E.; Chablo, A.; Howard, B. J. On the Structure of the Carbon Dioxide Dimer. *Chem. Phys. Lett.* **1979**, *60*, 414.

(18) Manuali, C.; Rampino, S.; Laganà, A. GriF: A Grid Framework for a Web Service Approach to Reactive Scattering. *Comput. Phys. Commun.* **2010**, *181*, 1179.

(19) Manuali, C.; Laganà, A. GriF: A New Collaborative Framework for a Web Service Approach to Grid Empowered Calculations. *Future Gen. Comp. Syst.* **2011**, *27*, 315.

(20) Faginas-Lago, N.; Lombardi, A.; Pacifici, L.; Costantini, A. Design and Implementation of a Grid Application for Direct Calculations of Reactive Rates. *Comp. Theor. Chem.* **2013**, *1022*, 103−107.

(21) Pacifici, L.; Verdicchio, M.; Faginas-Lago, N.; Lombardi, A.; Costantini, A. A High-Level Ab Initio Study of the N_2+N_2 Reaction Channel. *J. Comp. Chem.* **2013**, DOI: 10.1002/jcc.23415.

(22) COMPCHEM Virtual Organization, http://www.compchem.unipg.it; Laganà, A., Riganelli, A., Gervasi, O. In *Lect. Notes Comput. Sci.*, **2006**, *665*, 3980.

(23) Elango, G. S.; Maciel, G.; Lombardi, A.; Cavalli, S.; Aquilanti, V. Quantum Chemical and Dynamical Approaches to Intra and Intermolecular Kinetics: the $C_nH_{2n}O$ (n=1,2,3) Molecules. *Int. J. Quantum Chem.* **2011**, *111*, 1784−91.

(24) Elango, M.; Maciel, G. S.; Palazzetti, F.; Lombardi, A.; Aquilanti, V. Quantum Chemistry of C_3H_6O Molecules: Structure and Stability, Isomerization Pathways, and Chirality Changing Mechanisms. *J. Phys. Chem. A* **2010**, *114*, 9864−9874.

(25) Lombardi, A.; Palazzetti, F.; Maciel, G. S.; Aquilanti, V.; Sevryuk, M. B. Simulation of Oriented Collision Dynamics of Simple Chiral Molecules. *Int. J. Quantum Chem.* **2011**, *111*, 1651.

(26) Lombardi, A.; Maciel, G. S.; Palazzetti, F.; Grossi, G.; Aquilanti, V. Alignment and Chirality in Gaseous Flows. *J. Vacuum Soc. Japan* **2010**, *53*, 645.

(27) Aquilanti, V.; Grossi, G.; Lombardi, A.; Maciel, G. S.; Palazzetti, F. The origin of Chiral Discrimination: Supersonic Molecular Beam Experiments and Molecular Dynamics Simulations of Collisional Mechanisms. *Phys. Scr.* **2008**, *78*, 058119.

(28) Su, T.-M.; Palazzetti, F.; Lombardi, A.; Grossi, G.; Aquilanti, V. Molecular Alignment and Chirality in Gaseous Streams and Vortices. *Rendiconti Lincei* **2013**, *24*, 291.

(29) Lin, K.-C.; Kasai, T.; Nakamura, N.; Tsai, P.-Y.; Che, D.-C.; Aquilanti, V.; Lombardi, A.; Palazzetti, F. Aligned Molecules: Chirality Discrimination in Photodissociation and in Molecular Dynamics. *Rendiconti Lincei* **2013**, *24*, 299.

(30) Barreto, P. R. P.; Albernaz, A. F.; Capobianco, A.; Palazzetti, F.; Lombardi, A.; Grossi, G.; Aquilanti, V. Potential Energy Surfaces for Interactions of H_2O with H_2, N_2 and O_2: a Hyperspherical Harmonics Representation, and a Minimal Model for the H2O "rare-gas-atom Systems. *Comput. Theor. Chem.* **2012**, *990*, 53−61.

(31) Barreto, P. R. P.; Albernaz, A.; F.; Palazzetti, F.; Lombardi, A.; Grossi, G.; Aquilanti, V. Hyperspherical Representation of Potential Energy Surfaces: Intermolecular Interactions in Tetra-atomic and Penta-atomic Systems. *Phys. Scr.* **2011**, *84*, 028111.
(32) Aquilanti, V.; Grossi, G.; Lombardi, A.; Maciel, G. S.; Palazzetti, F. Aligned Molecular Collisions and a Stereodynamical Mechanism for Selective Chirality. *Rendiconti Lincei* **2011**, *22*, 125.
(33) Palazzetti, F.; Munusamy, E.; Lombardi, A.; Grossi, G.; Aquilanti, V. Spherical and Hyperspherical Representation of Potential Energy Surfaces for Intermolecular Interactions. *Int. J. Quantum Chem.* **2011**, *111*, 318−332.
(34) Barreto, P. R. P.; Palazzetti, F.; Grossi, G.; Lombardi, A.; Maciel, G. S.; Vilela, A. F. A. Range and Strength of Intermolecular Forces for van der Waals Complexes of the Type H_2X_n-Rg, with X = O, S and n = 1,2. *Int. J. Quantum Chem.* **2010**, *110*, 777.
(35) Aquilanti, V.; Lombardi, A.; Yurtsever, E. Global View of Classical Clusters: the Hyperspherical Approach to Structure and Dynamics. *Phys. Chem. Chem. Phys.* **2002**, *4*, 5040−51.
(36) Sevryuk, M. B.; Lombardi, A.; Aquilanti, V. *Phys. Rev. A* **2005**, *72*, 033201.
(37) Barreto, P. R. P.; Vilela, A. F. A.; Lombardi, A.; Maciel, G. S.; Palazzetti, F.; Aquilanti, V. The Hydrogen Peroxide-Rare Gas Systems: Quantum Chemical Calculations and Hyperspherical Harmonic Representation of the Potential Energy Surface for Atom-Floppy Molecule Interactions. *J. Phys. Chem. A* **2007**, *111*, 12754.
(38) Aquilanti, V.; Lombardi, A.; Sevryuk, M. B. Phase-space invariants for aggregates of particles: Hyperangular Momenta and Partitions of the Classical Kinetic Energy. *J. Chem. Phys.* **2004**, *121*, 5579−5589.
(39) Calvo, F.; Gadéa, X.; Lombardi, A.; Aquilanti, V. Isomerization Dynamics and Thermodynamics of Ionic Argon Clusters. *J. Chem. Phys.* **2006**, *125*, 114307.
(40) Carter, S.; Murrell, J. N. Analytical Two-valued Potential Energy Functions for the Ground State Surfaces of $CO_2(x^1\mathring{a}_g^+)$ and $CS_2(x^1\mathring{a}_g^+)$. *Croat. Chem. Acta* **1984**, *57*, 355.
(41) Pirani, F.; Cappelletti, D.; Liuti, G. Range, Strength and Anisotropy of Intermolecular Forces in Atom-molecule Systems: an Atom-bond Pairwise Additivity Approach. *Chem. Phys. Lett.* **2001**, *350*, 286.
(42) Pirani, F.; Albertí, M.; Castro, A.; Moix Teixidor, M.; Cappelletti, D. Atom-bond Pairwise Additive Representation for Intermolecular Potential Energy Surfaces. *Chem. Phys. Lett.* **2004**, *394*, 37.
(43) Siska, P. E.; Parson, J. M.; Schafer, T. P.; Lee, Y. T. Intermolecular Potentials from Crossed Beam Differential Elastic Scattering Measurements. III. He+He and Ne+Ne. *J. Chem. Phys.* **1971**, *55*, 5762.
(44) Farrar, J. M.; Lee, Y. T.; Goldman, V. V.; Klein, M. L. Neon Interatomic Potentials from Scattering Data and Crystalline Properties. *Chem. Phys. Lett.* **1973**, *19*, 359.
(45) Simons, G.; Parr, R. G.; Finlan, J. M. New Alternative to the Dunham Potential for Diatomic Molecules. *J. Chem. Phys.* **1973**, *59*, 3229.
(46) Bickes, R. W.; Bernstein, R. B. *Chem. Phys. Lett.* **1974**, *26*, 457.
(47) Bickes, R. W.; Bernstein, R. B. The SPF Dunham Expansion for the Potential Well: A Regression Model for Systematic Analysis of Differential Elastic Beam Scattering Cross Sections. *J. Chem. Phys.* **1977**, *66*, 2408.
(48) Hepburn, J.; Penco, R.; Scoles, G. A. Simple but Reliable Method for the Prediction of Intermolecular Potentials. *Chem. Phys. Lett.* **1975**, *36*, 451.
(49) Ahlrichs, R.; Penco, R.; Scoles, G. Intermolecular Forces in Simple Systems. *Chem. Phys.* **1977**, *19*, 119.
(50) Tang, K. T.; Toennies, J. P. An Improved Simple Model for the van der Waals Potential Based on Universal Damping Functions for the Dispersion Coefficients. *J. Chem. Phys.* **1984**, *80*, 3726.
(51) Pirani, F.; Brizi, S.; Roncaratti, L.; Casavecchia, P.; Cappelletti, D.; Vecchiocattivi, F. Beyond the Lennard-Jones Model: a Simple and Accurate Potential Function Probed by High Resolution Scattering Data Useful for Molecular Dynamics Simulations. *Phys. Chem. Chem. Phys.* **2008**, *10*, 5489.
(52) Maitland, G. C.; Smith, E. B. A Simplified Representation of Intermolecular Potential Energy. *Chem. Phys. Lett.* **1973**, *22*, 443.
(53) Lombardi, A.; Palazzetti, F. A Comparison of Interatomic Potentials for Rare Gas Nanoaggregates. *THEOCHEM* **2008**, *852*, 22.
(54) Pirani, F.; Maciel, G.; Cappelletti, D.; Aquilanti, V. Experimental Benchmarks and Phenomenology of Interatomic Forces: Open-shell and Electronic Anisotropy Effects. *Int. Rev. Phys. Chem.* **2006**, *25*, 165−199.
(55) Faginas-Lago, N.; Huarte-Larrañaga, F.; Albertí, M. On the Suitability of the ILJ Function to Match Different Formulations of the Electrostatic Potential for Water-water Interactions. *Eur. Phys. J. D* **2009**, *55*, 75−85.
(56) Albertí, M.; Faginas-Lago, N.; Pirani, F. Benzene Water Interaction: From Gaseous Dimers to Solvated Aggregates. *Chem. Phys.* **2012**, *399*, 232.
(57) Albertí, M.; Faginas-Lago, N. Ion Size Influence on the Ar Solvation Shells of Mi^+-C_6F_6 Clusters (M = Na, K, Rb, Cs). *J. Phys. Chem. A* **2012**, *116*, 3094.
(58) Albertí, M.; Aguilar, A.; Lucas, J. M.; Pirani, F.; Coletti, C.; Re, N. AtomâĹŠBond Pairwise Additive Representation for Halide Benzene Potential Energy Surfaces: an Ab Initio Validation Study. *J. Phys. Chem. A* **2009**, *113*, 14606.
(59) Albertí, M.; Faginas-Lago, N. Competitive Solvation of K+ by C_6H_6 and H_2O in the K^+-$(C_6H_6)_n$-$(H_2O)_m$ (n = 1−4; m = 1−6) Aggregates. *Eur. Phys. J. D* **2013**, *67*, 73.
(60) Maciel, G. S.; Barreto, P. R. P.; Palazzetti, F.; Lombardi, A.; Aquilanti, V. A Quantum Chemical Study of H_2S_2: Intramolecular Torsional Mode and Intermolecular Interactions with Rare Gases. *J. Chem. Phys.* **2008**, *129*, 164302.
(61) Ragni, M.; Lombardi, A.; Pereira Barreto, P. R.; Peixoto Bitencourt, A. C. Orthogonal Coordinates and Hyperquantization Algorithm. The NH_3 and H_3O^+ Umbrella Inversion Levels. *J. Phys. Chem. A* **2009**, *113*, 15355.
(62) Pack, R. T.; Berg, O. J.; El-Sayed, M. A. The symmetry of the 6.2 eV Two-photon Rydberg State in Hexatriene from the Polarization Properties of the Multiphoton Ionization Spectrum. *Chem. Phys. Lett.* **1978**, *55*, 197.
(63) Candori, R.; Pirani, F.; Vecchiocattivi, F. The N_2Ar Potential Energy Surface. *Chem. Phys. Lett.* **1983**, *102*, 412.
(64) Beneventi, L.; Casavecchia, P.; Volpi, G. G. High-resolution Total Differential Cross Sections for Scattering of Helium by O_2, N_2, and NO. *J. Chem. Phys.* **1986**, *85*, 7011.
(65) Beneventi, L.; Casavecchia, P.; Pirani, F.; Vecchiocattivi, F.; Volpi, G. G.; Brocks, G.; van der Avoird, A.; Heijmen, B.; Reuss, J. The Ne-O_2 Potential Energy Surface from High Resolution Diffraction and Glory Scattering Experiments and from the Zeeman Spectrum. *J. Chem. Phys.* **1991**, *95*, 195.
(66) Gomez, L.; Bussery-Honvault, B.; Cauchy, T.; Bartolomei, M.; Cappelletti, D.; Pirani, F. Global Fits of New Intermolecular Ground State Potential Energy Surfaces for N_2-H_2 and N_2-N_2 van der Waals Dimers. *Chem. Phys. Lett.* **2007**, *445*, 99.
(67) Hase, W. L.; Duchovic, R., J.; Hu, X.; Komornicki, A.; Lim, K. F.; Lu, D.-H.; Peslherbe, G. H.; Swamy, K. N.; Vande Linde, S. R.; Zhu, L.; Varandas, A.; Wang, H.; Wolf, R. J. *J. Quantum Chemistry Program Exchange Bulletin* **1996**, *16*, 671.